FDTD Analysis of Dielectric Resonators with Curved Surfaces

Noriaki Kaneda, Bijan Houshmand, and Tatsuo Itoh

***Abstract*— In this paper, the finite-difference time-domain (FDTD) method is applied to calculate the resonant frequency of dielectric resonators (DR's) with curved surface. The contour-path integral FDTD (CFDTD) is modified to deal with the curved surface of the dielectric body while the traditional rectangular cells are maintained. Results are compared with theoretical values and staircase approximation, and show that the present method is more accurate than the staircase approximation.**

***Index Terms*—Dielectric resonator, FDTD.**

I. Introduction

Dielectric resonators (DR's) and DR antennas have been analyzed by the finite-difference time-domian (FDTD) method by a number of authors [1]–[4]. It is found that the FDTD is well suited for these types of problems. For the axially symmetric structures, the resonant frequency and the intrinsic quality factor of the cylindrical DR has been successfully obtained by reducing three-dimensional (3-D) Maxwell's equations to two-dimensional (2-D) ones, and using rectangular grids in the 2-D computation domain. Those methods have simplicity and comparable accuracy to frequency-domain methods. However, in practice, the practical structures are often axially asymmetric, such as rod DR's with a rectangular coupling aperture for the dual-mode filters [5] and microstrip line-fed DR antennas [6], [7]. Therefore, the study of these structures by 3-D analysis is essential. In addition, a direct treatment of curved surfaces is required, since many practical structures contain such boundaries.

The contour-path integral FDTD (CFDTD) method has been successfully applied to curved surfaces of conducting and dielectric bodies [8], [9]. However, this method needs special treatment for those E-fields across the boundary such as the borrowing of neighboring fields [8] and the interpolation of fields [9]. These procedures cause additional complexity and computation time. Finite-volume time-domain (FVTD) techniques [10], [11] and the nonorthogonal FDTD method [12] have improved accuracy for the approximation of curved surfaces at the expense of complex operation and increased computation time and memory.

The method employed in this paper can also be classified as one form of the FVTD technique which is specifically applied on the traditional Yee's cell. In this paper, the idea of the effective dielectric constant is proposed to modify the CFDTD method, and to simplify the FVTD technique, to deal with curved dielectric surfaces. By doing so, no increase in computation time and memory is required as compared to the traditional FDTD method with staircase approximation. Finally, the method is applied for calculation of various DR structures. The results verify improved accuracy of the proposed method.

Manuscript received September 12, 1996; revised March 27, 1997.

N. Kaneda was with the Department of Electrical Engineering, Doshisha University, Tanabe, Kyoto 61003, Japan. He is now with the Department of Electrical Engineering, University of California at Los Angeles (UCLA), Los Angeles, CA 90095 USA.

B. Houshmand is with the Jet Propulsion Laboratory, Pasadena, CA 91109 USA.

T. Itoh is with the Department of Electrical Engineering, University of California at Los Angeles (UCLA), Los Angeles, CA 90095 USA.

Publisher Item Identifier S 0018-9480(97)06072-9.

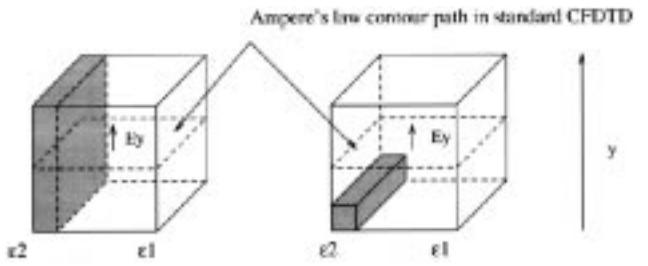

Fig. 1. Uniformally and nonuniformally filled dielectric material in one cell.

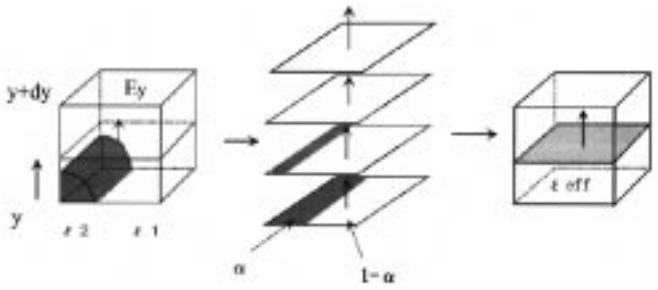

Fig. 2. Average of the electric-flux density.

II. The Effective Dielectric Constants

The conventional FDTD scheme cannot accommodate a partially filled dielectric material in one cell. Standard CFDTD can improve this problem when the dielectric is uniformly filled in one cell by applying the contour-path integral at a central plane of a cell [Fig. 1(a)] and by obtaining effective dielectric constants. However, if one cell is nonuniformly filled by a dielectric material [Fig. 1(b)], the contour-path integral at the central plane does not contain any more information of boundaries of different materials in one cell. When we deal with the curved surface with rectangular grids, cells around the curved surfaces are inevitably filled nonuniformly with dielectric materials. Thus, it is necessary to think of the electric field throughout the one cell. In order to do so, we take the average of the electric fields of different planes [Fig. 2(b)], and obtain the effective dielectric constant for one cell [Fig. 2(c)]. This is equivalent to the following procedure, starting from the Ampere's law

$$\frac{\partial}{\partial t}\int_A \vec{D}\, d\vec{A} = \oint_C \vec{H}\, d\vec{l} \tag{1}$$

which can be discretized on each plane of Fig. 2(b) as

$$\left(\frac{D_y|^{n+1}_{i,j,k} - D_y|^{n}_{i,j,k}}{\Delta t}\right)\cdot \Delta_x \Delta_z = (H_x|^{n+1/2}_{i,j,k+1/2} - H_x|^{n+1/2}_{i,j,k-1/2})\Delta_x - (H_z|^{n+1/2}_{i+1/2,j,k} - H_z|^{n+1/2}_{i-1/2,j,k})\Delta_z. \tag{2}$$

Since the electric fields parallel to the boundary of two different materials are continuous on each plane, the electric-flux density (D_y) at each plane of Fig. 2(b) can be expressed as

$$D_y = (\epsilon_2 \alpha(y) + \epsilon_1(1-\alpha(y)))\cdot E_y \tag{3}$$

where α is the fraction of the material of dielectric constant ϵ_2 in the cross section of a cell [Fig. 2(b)]. Since the vertical components of the electric fields along the boundary of different materials are not

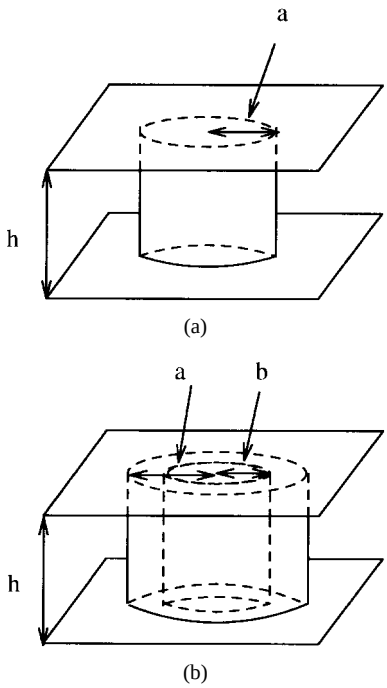

Fig. 3. (a) Rod and (b) ring DR sandwiched between two parallel conducting plates.

continuous, E_y on the different planes has different values. Hence, we take the average of the electric fields to the axial direction (y-direction)

$$\frac{1}{\Delta y}\int_y^{y+\Delta y} E_y^{n+1}\,dy = \frac{1}{\Delta y}\int_y^{y+\Delta y} E_y^{n}\,dy + \frac{1}{\Delta y}\int_y^{y+\Delta y}\frac{1}{\epsilon_2\alpha(y)+\epsilon_1(1-\alpha(y))}\,dy \cdot \begin{pmatrix} H_x|_{i,j,k+1/2}^{n+1/2} - H_x|_{i,j,k-1/2}^{n+1/2})\dfrac{\Delta t}{\Delta z} \\ -(H_z|_{i+1/2,j,k}^{n+1/2} - H_z|_{i-1/2,j,k}^{n+1/2})\dfrac{\Delta t}{\Delta x}\end{pmatrix}. \quad (4)$$

By letting

$$\frac{1}{\Delta y}\int_y^{y+\Delta y} E_y^{n+1}\,dy \rightarrow E_y|_{i,j,k}^{n+1} \quad (5)$$

(4) is now the same as the usual curl equation of Maxwell's equations, except for the dielectric constants. The effective dielectric constant used here is

$$\epsilon_y^{\text{eff}} = \left[\frac{1}{\Delta y}\int_y^{y+\Delta y}\frac{1}{\epsilon_2\alpha(y)+\epsilon_1(1-\alpha(y))}\,dy\right]^{-1}. \quad (6)$$

By repeating the above procedures for the rest of the components of the electric flux and throughout the curved surfaces, all the information of the curved surfaces of the dielectric body are contained in the position-dependent effective dielectric constant. These procedures are carried out before the FDTD-method time marching starts. Therefore, no additional correction is required in the time-marching loop, unlike the usual CFDTD method. The coincidence of grids and actual geometry is not even required because the boundaries inside the cells are taken care of while simple rectangular grids are maintained. Because the only difference between the present and the conventional FDTD method is the estimates of the effective dielectric constants, the present method has the same stability as the conventional FDTD method.

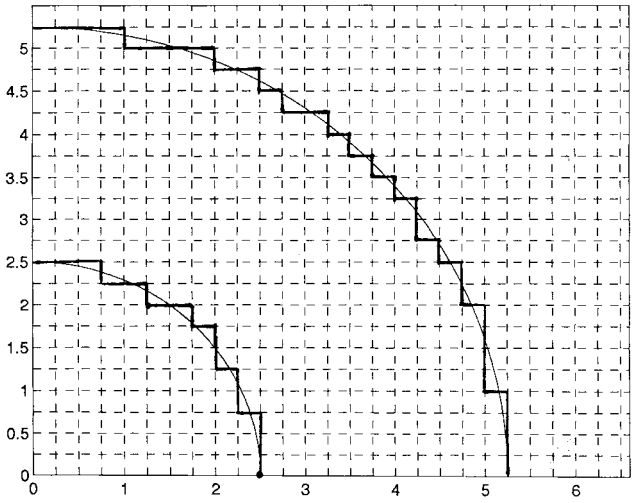

Fig. 4. Staircase grid ($\Delta x = \Delta y = 0.25$ mm).

Since the original Yee's grid and algorithm are used, the electric-flux conservation as well as the magnetic-flux conservation is maintained even though the effective dielectric constants are introduced. The electric-flux density over the surface of one Yee cell is equal to zero as follows:

$$\frac{\partial}{\partial t}\oint_{\text{cell}} \vec{D}\cdot\vec{S} = 0 \quad (7)$$

which can readily be shown by the same procedure because of the proof of the divergence-free nature of the free-space Yee cell [13].

III. Results

A. Resonant Frequency

The present method is applied to two structures to show accuracy of the method: one is the resonant frequency of a dielectric-rod resonator sandwiched between two parallel conducting plates and the other is the resonant frequency of a dielectric-ring resonator also sandwiched between two parallel conducting plates.

To verify the accuracy of the present method, the resonant frequencies of the structures in Fig. 3 are calculated by the 3-D FDTD method with the present method, the 3-D FDTD method with staircase approximation, and the 2-D FDTD method [1] and theoretical method with modal expansion. For the simulation by the 3-D FDTD method with the present method, Mur's second-order absorbing-boundary condition is used for the outer boundaries. Excitation is supplied with the modulated Gaussian pulse as a unit element source inside the DR's. Observation of modes is carried out by avoiding nodal points of each modes. The staircase approximation for those structures is shown in Fig. 4. For the simulation by the 2-D FDTD method in which the cylindrical coordinates are reduced to the two dimensions, the ABC for the Cartesian coordinates like Mur's ABC cannot directly be used. Therefore, the Kirchoff's solution of the wave equation [1] is used for the radiation boundaries. For the singular-value field elements at $r = 0$, which is one end of the computational domain, odd and even symmetry of fields in terms of the z-axis in the r–z plane is assumed depending on the odd and even axial modes. The ABC is located at the distance sufficiently far from the surface of the DR where the ABC location does not affect the resonant frequencies any more. Since the fields outside the DR are quickly decaying, the ABC can be placed rather close to the DR surface. For the 2-D FDTD method, the ABC is located at $5a$ (a is the radii of the DR) away from the surface of the DR, while the ABC for the 3-D

TABLE I
RESONANT FREQUENCIES OF A PARALLEL-PLATE DIELECTRIC-ROD RESONATOR [FIG. 3(a)]

Mode	Resonant frequency f(GHz)				Mesh Size	error(%)
	Theoretical	Present	Staircase	2D-FDTD		
HEM_{111}	6.214	6.21	6.20	6.21	$\lambda/27$	0.06
HEM_{211}	7.514	7.51	7.49	7.51	$\lambda/22$	0.05
HEM_{311}	9.003	8.99	8.97	9.00	$\lambda/18$	0.14
HEM_{131}	9.499	9.47	9.44	9.48	$\lambda/17$	0.30
HEM_{221}	9.726	9.74	9.68	9.72	$\lambda/17$	0.14
HEM_{411}	10.579	10.56	10.52	10.58	$\lambda/16$	0.18

TABLE II
RESONANT FREQUENCIES OF A PARALLEL-PLATE DIELECTRIC-RING RESONATOR [FIG. 3(b)]

Mode	Resonant frequency f(GHz)				Mesh Size	error(%)
	Theoretical	Present	Staircase	2D-FDTD		
HEM_{111}	7.452	7.46	7.49	7.45	$\lambda/26$	0.11
HEM_{211}	8.144	8.15	8.18	8.14	$\lambda/24$	0.07
HEM_{311}	9.321	9.32	9.34	9.32	$\lambda/22$	0.01
HEM_{121}	10.525	10.52	10.56	10.50	$\lambda/19$	0.05
HEM_{411}	10.739	10.73	10.77	10.74	$\lambda/19$	0.08

TABLE III
RESONANT FREQUENCIES OF $HEM_{11\delta}$ OF A DIELECTRIC-ROD RESONATOR IN A RECTANGULAR CAVITY (FIG. 5)

Size		Resonant frequencies f(GHz)		
2R(inch)	t(inch)	Present	Mode Matching [14]	Measured[14]
0.654	0.218	4.40	4.3880	4.382
0.689	0.230	4.17	4.1605	4.153
0.757	0.253	3.78	3.721	3.777

FDTD method is located at approximately $3a$ from the surface of the DR. Since the Kirchoff's radiation condition is equivalent to the Mur's first-order boundary condition in the approximation order, the distance to the ABC from the DR surface should be made larger in the 2-D simulation rather than in the 3-D simulation. Time-domain data of the FDTD method are all transformed to frequency-domain data by the discrete time Fourier transform (DTFT), which is the numerical integration of the Fourier transform, where the resonant frequencies are obtained from the peaks of the frequency response. More discussions about the application of the DTFT to FDTD time-domain data can be found in [3].

Table I shows the simulation results of the rod DR [Fig. 3(a)]. The mesh size used here is the same for all methods and modes. Therefore, relative mesh size differs among different frequencies. λ in Table I refers to the wavelength in the dielectric media at resonant frequencies. The error in Table I is the discrepancy between the results by the present method and the theoretical values. The present method predicts more accurate resonant frequencies compared to the staircase approximation. Since in the 2-D FDTD method the angular mode is analytically taken care of, the 2-D FDTD can predict accurate results for angularly higher order modes such as HEM_{311} and HEM_{411}. In the results shown in Table II, the improved accuracy of the present method over the staircase method is apparent. For example, for the HEM_{111} mode, even though the mesh size is very small in terms of the wavelength $(\lambda/26)$, the staircase method has more than 0.5% discrepancy to the theoretical value while the present method has about 0.1% error. Since DR's are used for very narrow-bandwidth application such as the DR filters with approximately 1% passband bandwidth [5] (due to its high Q nature and adjacent spurious modes), these errors caused by the staircasing of dielectric materials are not insignificant. Since the curvature (1/(radius) for the circle) of the inner circle of the ring resonator is large in terms of wavelength, it is very difficult for the staircase method to accurately approximate boundaries (Fig. 4), whereas the present method has no difficulties in doing so.

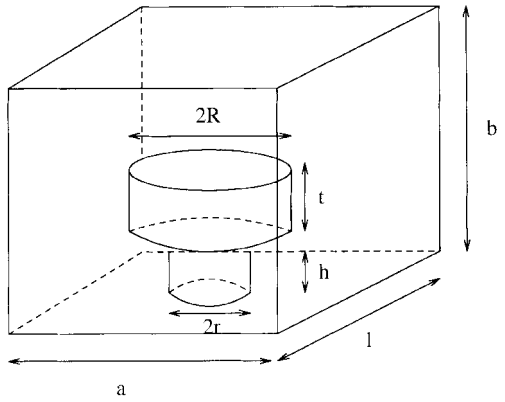

Fig. 5. Rod DR in a rectangular cavity.

Table III shows the resonant frequencies of the $HEM_{11\delta}$ mode for the different size of the dielectric rod resonator in a rectangular cavity (Fig. 5). The support of the DR is assumed to have the dielectric constant $\epsilon_r = 1$ in this simulation. The mesh size used here is about $\lambda/25$, where λ is again the wavelength in the dielectric media at resonant frequency. The results are compared with the mode-matching simulation data and the measured data from [14]. Overall good agreement is observed, despite a slight discrepancy at (and greater than) the third digit between the present method and the mode-matching method. As previously confirmed, the present method can be assured to have accuracy up to three digits.

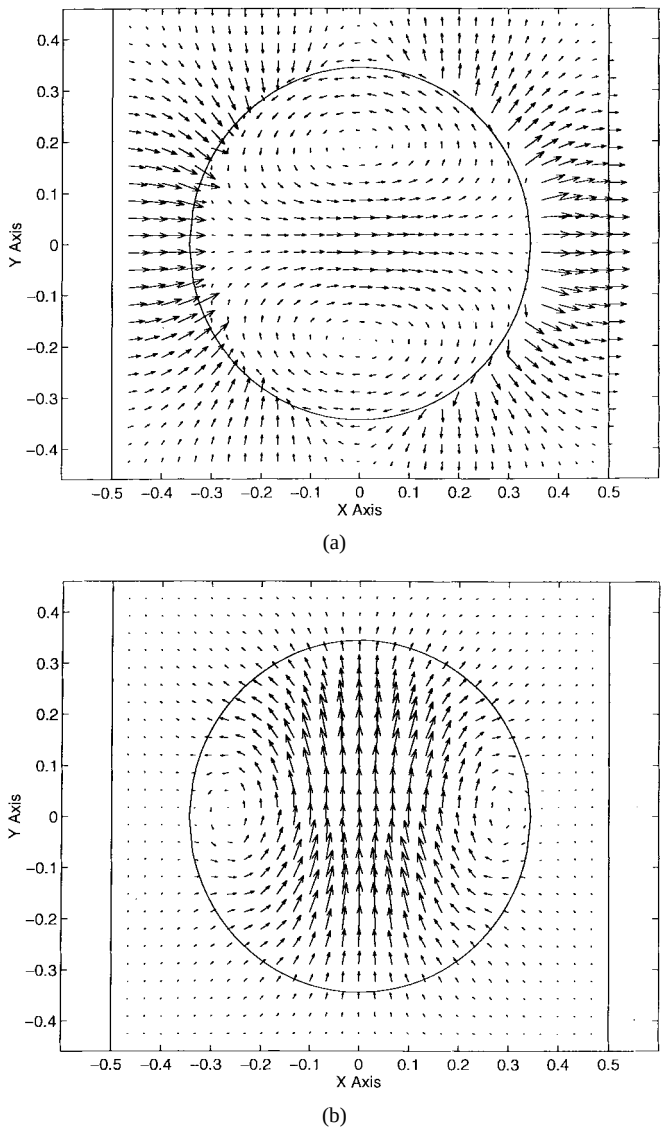

(a)

(b)

Fig. 6. (a) Electric-field distribution ($\mathrm{HEM}_{11\delta}$ mode). (b) Magnetic-field distribution ($\mathrm{HEM}_{11\delta}$ mode).

The calculation of the quality factor requires long computation time before the convergence is reached [2]. Therefore, a combination of the FDTD method with one of the spectrum estimation techniques is desired to obtain the quality factor of the DR's [2], [3].

B. Modal-Field Distribution

The peaks of the FDTD frequency response do not provide any information about resonant modes. The designation of resonant modes are meaningless in the 3-D FDTD method, because there is no modal-field expansion in the procedure. However, one needs to know the modal-field distributions for some applications, such as mutual coupling of certain modes of the DR's. Although the calculation of a single modal distribution is nearly impossible in the time-domain method, we can obtain a general idea of a modal-field distribution by exciting the DR at a resonant frequency and carefully choosing the excitation point. The determination of the excitation point is the main task for the FDTD method to obtain a modal-field distribution. The cut-and-try procedure is inevitable if we do not have any knowledge about the field distribution which we try to obtain. Consultation with the literature [14], [15] would be helpful to obtain general ideas of field distributions of DR's even in the case where the structure is different. The modal-field distributions for Fig. 5 are obtained in Fig. 6(a) and (b). The fields are excited at 4.134 GHz for the size of $2a = 1''$, $b = 1''$, $l = 0.92''$, $2r = 0''$, $2R = 0.689''$, $t = 0.230''$, and $\epsilon = 38$. The excitation point is placed inside the DR to obtain faster convergence. The results agree well with the field distribution drawn by the mode-matching method [14].

IV. Conclusion

The resonant frequencies of DR's are calculated by the FDTD method. The simpler algorithm with the concept of the effective dielectric constants is introduced to more accurately deal with the curved surfaces of the DR's. The method is verified by comparing the results with the theoretical values of the parallel-plate dielectric-rod and dielectric-ring resonators. The method introduced has an advantage over the staircase approximation in terms of accuracy and over the other CFDTD, FVTD, and nonorthogonal FDTD methods, in terms of the simpler and faster FDTD computation. From the simulation of the dielectric-ring resonator, the staircase FDTD is found to generate intolerable errors caused by the curved surface of the large curvature in terms of wavelength. The DR loaded rectangular-cavity structure where the 2-D FDTD method cannot be applied is also analyzed by using the present method. The results are compared with the mode-matching and measured data, with good agreement achieved.

References

[1] A. Navarro and M. J. Nuñez, "FDTD method coupled with FFT: A generalization to open cylindrical devices," *IEEE Trans. Microwave Theory Tech.*, vol. 42, pp. 868–874, May 1994.

[2] J. A. Pereda, L. A. Vielva, A. Vegas, and A. Prieto, "Computation of resonant frequencies and quality factors of open dielectric resonators by a combination of the finite-difference time-domain (FDTD) and Prony's methods," *IEEE Microwave Guided Wave Lett.*, vol. 2, pp. 431–433, Nov. 1992.

[3] Z. Bi, Y. Shen, K. Wu, and J. Litva, "Fast finite-difference time-domain analysis of resonators using digital filtering and spectrum estimation techniques," *IEEE Trans. Microwave Theory Tech.*, vol. 40, pp. 1611–1619, Aug. 1992.

[4] S. M Shum and K. M Luk, "Analysis of aperture coupled rectangular dielectric resonator antenna," *Electron. Lett.*, vol. 30, pp. 1726–1727, Oct. 1994.

[5] C. Wang, H. W. Yao, K. A. Zaki, and R. R. Mansour "Mixed modes cylindrical planar dielectric resonator filters with rectangular enclosure," *IEEE Trans. Microwave Theory Tech.*, vol. 43, pp. 2817–2822, Dec. 1995.

[6] A. A. Kishk, A. Ittipiboon, Y. M. M. Antar, and M. Cuhaci, "Slot excitation of the dielectric disk radiator," *IEEE Trans. Antennas Propagat.*, vol. 43, pp. 198–201, Feb. 1995.

[7] K. W. Leung, K. M Luk, K. Y. A. Lai, and D. Lin "Theory and experiment of an aperture-coupled hemispherical dielectric resonator antenna," *IEEE Trans. Antennas Propagat.*, vol. 43, pp. 1192–1198, Nov. 1995.

[8] T. G. Jurgens, A. Taflove, K. Umashankar, and T. G. Moore, "Finite-difference time-domain modeling of curved surfaces," *IEEE Trans. Antennas Propagat.*, vol. 40, pp. 357–365, Apr. 1992.

[9] K. S. Yee, J. S. Chen, and A. H. Chang, "Conformal finite-difference time-domain (FDTD) with overlapping grids," *IEEE Trans. Antennas Propagat.*, vol. 40, pp. 1068–1075, Sep. 1992.

[10] N. K. Madsen and R. W. Ziolkowski, "A three-dimensional modified finite volume technique for Maxwell's equations," *Electromagnetics*, vol. 10, pp. 147–161, 1990.

[11] K. S. Yee and J. S. Chen, "Conformal hybrid finite difference time domain and finite volume time domain," *IEEE Trans. Antennas Propagat.*, vol. 42, pp. 1450–1455, Oct. 1994.

[12] P. H. Harms, J. F. Lee, and R. Mittra, "A study of the nonorthogonal FDTD method versus the conventional FDTD technique for computing resonant frequencies of cylindrical cavities," *IEEE Trans. Microwave Theory Tech.*, vol. 40, pp. 741–746, Apr. 1992.

[13] A. Taflove, *Computational Electrodynamics: The Finite-Difference Time-Domain Method*. Norwood, MA: Artech House, 1995, pp. 76–77.
[14] X. P. Liang and K. A. Zaki, "Modeling of cylindrical dielectric resonators in rectangular waveguides and cavities," *IEEE Trans. Microwave Theory Tech.*, vol. 41, pp. 2174–2181, Dec. 1993.
[15] D. Kajfez, A. W. Guillon, and J. James, "Computed modal-field distributions for isolated dielectric resonators," *IEEE Trans. Microwave Theory Tech.*, vol. MTT-32, pp. 1609–1616, Dec. 1984.

A Pole-Free Modal Field-Matching Technique for Eigenvalue Problems in Electromagnetics

Smain Amari and Jens Bornemann

***Abstract*— A pole-free formulation of the modal field-matching technique (MFMT) as applied to eigenvalue problems in electromagnetics is presented in this paper. The poles in the determinantal equation are systematically *eliminated*, without requiring previous knowledge of their locations or nature, resulting in well-behaved determinants. The minimum singular value in a singular-value decomposition of the pole-free matrix exhibits much wider dips than what is obtained from the standard MFMT. The pole-free formulation is applied to determine the cutoff wavenumbers of a ridged waveguide to demonstrate its validity and efficiency.**

***Index Terms*— Eigenvalues/eigenfunctions, mode-matching methods, ridge waveguides.**

I. Introduction

A large number of problems in engineering, physics, and applied mathematics are reduced to solving a homogeneous matrix equation of the form

$$[A(k)][x] = 0 \tag{1}$$

where $[A(k)]$ is a parameter-dependent square complex matrix of order $n \times n$ and x is an unknown n-element column vector [1], [2]. Nontrivial solutions to (1) exist only when the matrix $[A]$ is singular, i.e., when its determinant vanishes for certain values of the parameter k:

$$\det[A(k)] = 0, \qquad k = k_0. \tag{2}$$

The numerical solution of (2) is often hindered by the presence of poles in the determinant in the vicinity of its zeros, thereby leading to a time-consuming search and nonphysical roots. This situation is often encountered in the application of the modal field-matching technique (MFMT) to determining cutoff frequencies and propagation constants of microwave and millimeter-wave structures.

A few attempts have been made to eliminate poles from specific applications in the recent years. In [3], a pole–zero combination was used in the determination of spectrum of unilateral finline. In [4], a pole-free function was constructed once the locations of the poles were determined. In both approaches, the accurate determination of the pole locations is required in a first step in order to reliably detect the zeros in the second step.

Manuscript received October 29, 1996; revised March 7, 1997.

The authors are with the Laboratory for Lightwave Electronics, Microwaves and Communications, LLiMiC, Department of Electrical and Computer Engineering, University of Victoria, Victoria, B.C., Canada V8W 3P6.

Publisher Item Identifier S 0018-9480(97)06073-0.

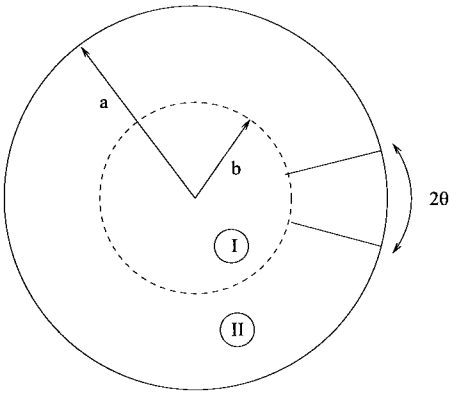

Fig. 1. Cross section of a ridged circular waveguide.

A direct way in avoiding the poles consists of maintaining the original equations as obtained from the boundary conditions. The large size of the resulting matrix requires large central processing unit (CPU) times especially when large numbers of modes are needed. When equal numbers of modes are retained in the modal expansions, it is possible to eliminate the poles from the determinantal equation. However, the resulting determinant is practically a rectangular function, thereby adding to the CPU times required to accurately locate its zeros [5].

A technique to circumvent these poles was presented by Labay and Bornemann where the singular-value decomposition of the matrix $[A(k)]$ is used instead of its determinant [6]. In this approach, nontrivial solutions to (1) are determined from the zeros of the smallest singular value in the singular-value decomposition of the matrix $[A(k)]$ [6].

It is important to note that this approach, despite its success in reformulating the problem through a pole-free quantity, does not eliminate the poles from the matrix $[A(k)]$. In fact, the poles in the determinant are reflected in the singular-value approach through the sharpness of the minima. The sharpness of a minimum in the smallest singular value increases as its location approaches a pole of the determinant. This will be shown by the numerical results of this paper.

Here we reexamine the origin of the poles in the determinant within the MFMT and show how they can be systematically eliminated from the matrix $[A(k)]$ without requiring prior knowledge of their locations. These poles result from the inversion of singular matrices in the construction of the matrix $[A(k)]$. By carefully avoiding such operations, we show how well-behaved determinants can be obtained. The resulting determinant is inherently pole-free and the minima of the smallest singular value are broader than in the standard MFMT.

II. A Pole-Free Modal Field-Matching Technique

We focus attention on the structure shown in Fig. 1. The ridge of thickness 2θ and depth $h = a - b$ and the metallic walls of the waveguide are assumed lossless. Here, we present only the analysis of the transverse-electric (TE) modes as these are sufficient to illustrate the approach.

The TE modes can be divided into two sets with either an electric or a magnetic wall along its plane of symmetry. The case of the electric-wall symmetry is treated in details, although numerical results for the cutoff wavenumbers will be given for both symmetries.